JACS
JOURNAL OF THE AMERICAN CHEMICAL SOCIETY
Communication
pubs.acs.org/JACS

Electrochemical Control of Single-Molecule Conductance by Fermi-Level Tuning and Conjugation Switching

Masoud Baghernejad,[†,#] Xiaotao Zhao,[‡,#] Kristian Baruël Ørnsø,[§,#] Michael Füeg,[†] Pavel Moreno-García,[†] Alexander V. Rudnev,[†] Veerabhadrarao Kaliginedi,[†] Soma Vesztergom,[†] Cancan Huang,[†] Wenjing Hong,*[,†] Peter Broekmann,[†] Thomas Wandlowski,[†] Kristian S. Thygesen,*[,§] and Martin R. Bryce*[,‡]

[†]Department of Chemistry and Biochemistry, University of Bern, Freiestrasse 3, CH-3012, Bern, Switzerland
[‡]Department of Chemistry, Durham University, Durham DH1 3LE, United Kingdom
[§]Center for Atomic-scale Materials Design, Department of Physics, Technical University of Denmark, 2800 Kgs. Lyngby, Denmark

Supporting Information

ABSTRACT: Controlling charge transport through a single molecule connected to metallic electrodes remains one of the most fundamental challenges of nanoelectronics. Here we use electrochemical gating to reversibly tune the conductance of two different organic molecules, both containing anthraquinone (AQ) centers, over >1 order of magnitude. For electrode potentials outside the redox-active region, the effect of the gate is simply to shift the molecular energy levels relative to the metal Fermi level. At the redox potential, the conductance changes abruptly as the AQ unit is oxidized/reduced with an accompanying change in the conjugation pattern between linear and cross conjugation. The most significant change in conductance is observed when the electron pathway connecting the two electrodes is via the AQ unit. This is consistent with the expected occurrence of destructive quantum interference in that case. The experimental results are supported by an excellent agreement with ab initio transport calculations.

Controlled switching between different charge-transport states of single-molecule components is one of the most essential and challenging aspects of molecular electronics. Conductance switching in molecular junctions has been demonstrated previously using various means, including light,[1] bias pulses,[2] electrostatic gating,[3] and electrochemical gating.[4] The concept of "electrochemical gating", which provides the opportunity to overcome the technical challenges of incorporating a gate electrode in a solid-state molecular device, has been employed in electrochemically active molecular systems, including viologens,[5] oligoaniline,[6] ferrocene,[7] transition metal complexes,[4b,8] perylenebisimides,[9] redox-active proteins,[10] quinones,[11] and tetrathiafulvalene,[12] as well as redox-inactive molecules.[13] In the case of redox-inactive molecules, or more generally when the electrode potential does not overlap with the molecule's redox potential, the effect of the gate is simply to shift the molecular levels up or down in energy relative to the Fermi level. In a simple picture where tunneling through the molecule is described by "Lorentzian" transmission peaks centered at the discrete energy levels of the molecule, a large on/off conductance ratio can be achieved by moving the frontier molecular level in and out of resonance with the Fermi level E_F.

Recently, the concept of quantum interference (QI) in molecular transport junctions has been introduced theoretically and verified experimentally.[14] Destructive QI leads to very low conductance—much lower than anticipated from a simple "Lorentzian" model treating each molecular level as an independent transport channel. It occurs as a result of a (nearly) complete cancellation of transmission probability due to interference between different electron pathways, and it is predicted to take place in organic molecules whenever the path connecting the left and right electrodes via the molecule is cross conjugated.[14a,15] For example, independent measurements show that the conductance of a cross-conjugated anthraquinone (AQ) is ∼100 times lower than that of a linearly conjugated anthracene,[14f,15,16] even though the molecular length, electronic energy levels, and optical properties of the two molecules are very similar.

In this work, two π-conjugated molecules, isomeric AQ-1,5 and AQ-1,4, with an anthraquinone core unit (Figure 1a), were synthesized, and their electronic conductance was measured under electrochemical gating using the scanning tunneling microscopy break-junction (STM-BJ) technique. We demonstrate gate potential control of the molecular energy levels over almost 1 eV with conductance variations of >1 order of magnitude. The origin of the conductance variation is a combined effect of continuous Fermi level tuning (for potentials outside the redox-active region) and abrupt changes to the conjugation pattern of the molecule as a consequence of oxidation/reduction of the molecule when the electrode potential crosses the redox potential. These experimental observations are complemented by density functional theory (DFT)-based transport calculations. Plotting the calculated transmission function of the reduced and oxidized molecule on the electrode potential scale, we find excellent agreement with experiments for the conductance versus gate potential in a 1 V range around the AQ redox potential.

Received: October 8, 2014
Published: December 15, 2014

dx.doi.org/10.1021/ja510335z | J. Am. Chem. Soc. 2014, 136, 17922−17925

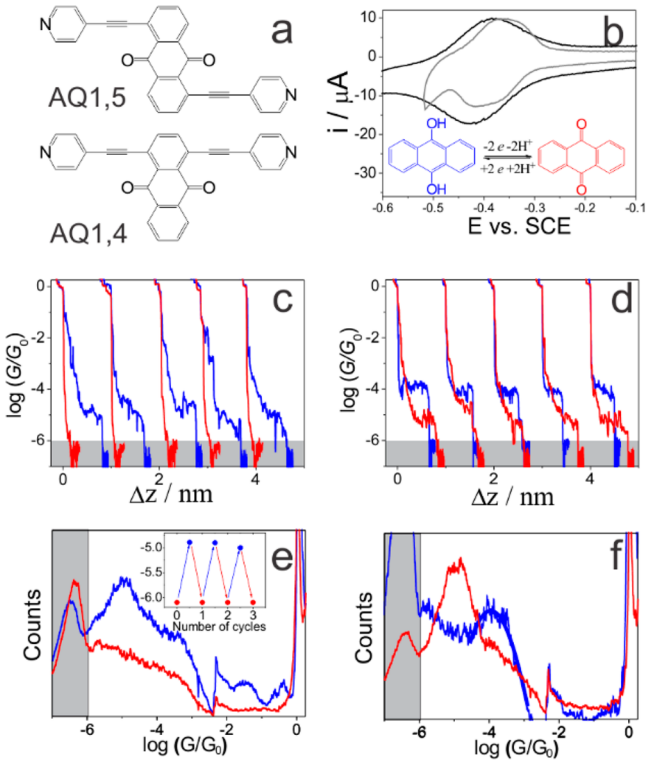

Figure 1. (a) The molecules studied in this work. (b) CV of AQ-1,5 (black) and AQ-1,4 (gray) assembly measured in the STM cell with sweep rate of 100 mV s^{-1} in 0.1 M $KClO_4$ aqueous electrolyte. Typical conductance vs distance traces of rAQ-1,5 (c, blue, −530 mV), AQ-1,5 (c, red, −280 mV), rAQ-1,4 (d, blue, −520 mV), AQ-1,4 (d, red, 280 mV) relative to SCE. (e,f) 1D conductance histograms generated from 1100 individual curves without any data selection for rAQ-1,5 (e, blue), AQ-1,5 (e, red), rAQ-1,4 (f, blue), and AQ-1,4 (f, red). (e, inset) Three sequential *in situ* highly reversible switching cycles between rAQ-1,5 and AQ-1,5 triggered by the electrode potential. The data points are the most probable conductances of rAQ-1,5 (blue) and AQ-1,5 (red). The noise level is indicated by the gray area in panels c–f. The spike at log $(G/G_0) \approx -2.2$ is the switching of the amplifier.

Conductance measurements of both AQ-1,4 and AQ-1,5 were performed in an STM-BJ setup in 0.1 M $KClO_4$ (pH ~5.8) using a cell with a four-electrode configuration, with Au as tip and substrate, and Pt wires as counter-electrode and quasi-reference electrode in an oxygen-free atmosphere (see SI).[17] Figure 1b shows the cyclic voltammogram (CV) of AQ-1,5 recorded in the STM cell. Two redox peaks are located around −0.42 V for AQ-1,5 and −0.37 V for AQ-1,4 (Figure 1b).

Figure 1c shows typical conductance–distance traces of AQ-1,5 in the reduced and oxidized states obtained from the STM-BJ experiment.[18] For both redox states, the conductance curves exhibit a short plateau at $1G_0$ due to atomic gold point contacts existing just before rupture. In addition to the $1G_0$ plateau, the blue curves show a more extended plateau, with conductances ranging from $10^{-4.6}G_0$ to $10^{-5.4}G_0$, which can be assigned to the conductance of the reduced AQ-1,5 single-molecule junctions. In contrast, no low-conductance plateaus were observed for AQ-1,5 in the oxidized state (red curve). From this, we conclude that the conductance of the oxidized form is below the detection limit of our STM-BJ setup equipped with a linear I–V convertor ($10^{-6}G_0$). Figure 1e shows the one-dimensional histograms of AQ-1,5 in its reduced (blue) and oxidized (red)

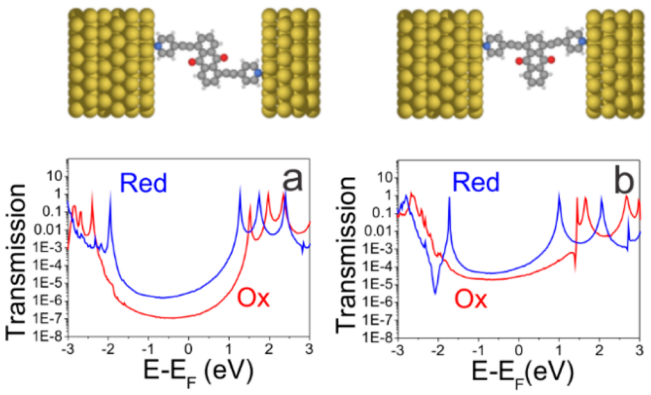

Figure 2. Calculated transmission function for the two charge states of AQ-1,5 (a) and AQ-1,4 (b). The supercells used for the transport calculations are also shown. The energy scale is relative to the Au Fermi level.

states, constructed from 1100 conductance traces without any data selection. A pronounced conductance peak centered at $10^{-5.0}G_0$ is observed for the reduced state (rAQ-1,5), while no clear peaks above the detection limit are found for the oxidized form. The inset of Figure 1e shows the change in conductance of AQ-1,5 over three consecutive cycles of the potential across the redox potential. No significant decrease of the on/off ratio is observed, which suggests that the manipulation of molecular redox states is a highly reversible process.

Figure 1d,f shows individual conductance–distance traces and histograms of AQ-1,4 in the reduced (blue) and oxidized (red) states, respectively. For this molecule, clear conductance plateaus are observed around $10^{-4.0}G_0$ and $10^{-5.0}G_0$ for the reduced and oxidized species, respectively, leading to peaks in the conductance histogram at these values. We attribute these peaks to the formation of rAQ-1,4 and AQ-1,4 single-molecule junctions.

The smaller difference in the conductance of the two redox states of AQ-1,4, compared to AQ-1,5, can be explained by the different electron pathways between the pyridyl units in the cross-conjugated AQ-1,5 and linearly conjugated AQ-1,4 molecules. For AQ-1,4 the change in conductance results primarily from a change in effective electron density of the functional group attached as a "gating" unit to the OPE-type backbone. In contrast, the electron pathway for AQ-1,5 goes directly via the AQ unit, and thus the change from linear- (reduced state) to cross-conjugation (oxidized state) directly lowers the transmission probability.

In Figure 2, we show the transmission functions of AQ-1,5 (a) and AQ-1,4 (b) in reduced and oxidized forms calculated from DFT. All the calculations were performed using the GPAW electronic structure[19] code using a double zeta plus polarization (DZP) basis set. To overcome the well-known problem of DFT to describe molecular energy levels we have used the DFT+ Sigma scheme to correct the DFT eigenvalues as described in previous studies.[20,21] More details on the computations are given in the SI. Our transport calculations predict that the oxidized states generally have lower conductance than the reduced states. This holds not only for energies at the gold Fermi level but over the entire range of energies within the HOMO–LUMO gap. Moreover, AQ-1,4 is predicted to have higher conductance than AQ-1,5 in both charge states. Finally, the change in conductance upon changing the redox state is predicted to be larger for AQ-1,5

dx.doi.org/10.1021/ja510335z | J. Am. Chem. Soc. 2014, 136, 17922–17925

than for AQ-1,4. These findings are all consistent with the experimental observations. The first two findings can be explained by the variations in the HOMO−LUMO gap: for both charge states the HOMO−LUMO gap is larger for AQ-1,5 than for AQ-1,4, and for both molecules the HOMO−LUMO gap is larger in the oxidized state than in the reduced state. However, the third finding, namely that the conductance change upon oxidation is larger for AQ-1,5 than for AQ-1,4, cannot be explained simply from the size of the HOMO−LUMO gap. Indeed, the increase in HOMO−LUMO gap upon oxidation is very similar for the two molecules. Instead, the larger suppression of the conductance in oxidized AQ-1,5 is a result of destructive QI occurring because the electron pathway connecting the left and right electrodes goes via the cross-conjugated AQ unit. We note that the QI effect is not very pronounced in oxidized AQ-1,5; in particular, the characteristic transmission anti-resonance often observed in QI molecules is not observed. Outside the redox-active region, the effect of the gate potential should simply shift the molecular levels up or down relative to the metal Fermi energy. Since the conductance is proportional to the transmission function at the Fermi energy, Figure 2 suggests that a significant gating effect should be observable when the Fermi level is close to either the HOMO or LUMO, and previous studies have shown that AQ-1,4 and AQ-1,5, in the absence of gating potentials, conduct through the LUMO.[22]

To investigate the conductance versus gate potential, we constructed conductance histograms for the two molecules at different (fixed) electrode potentials. The histograms are shown in Figure 3 for AQ-1,5 and AQ-1,4, and the conductance peaks versus gate potential are plotted in Figure 4a,b. For potentials higher than the redox potential, the molecules are in their oxidized state. In this potential region, the peaks in the conductance histograms shift to higher conductance as the potential is moved toward more negative values (the Fermi level is moved upward). This indicates that transport is indeed mediated by the LUMO for the oxidized molecules. At a potential around −0.4 V vs SCE, the conductance increases sharply by approximately 1 order of magnitude due to the redox process. For AQ-1,5 the conductance continues to rise as the potential is decreased further, indicating that transport is also LUMO-mediated in the reduced state. A significant conductance change from $10^{-6.1}G_0$ (−330 mV vs SCE) to $10^{-6.5}G_0$ (−30 mV vs SCE) for AQ-1,5 in the oxidized state was observed by carrying out the experiment in a complementary STM-BJ with a developing logarithm $I-V$ convertor with better current sensitivity, which is in good agreement with the results presented in Figure 1, showing that the oxidized state conductance of AQ-1,5 is $<10^{-6}G_0$. For AQ-1,4, it is found that the conductance increases with positive potential in the reduced state. At the potential close to redox potential (−420 mV vs SCE), we can still observe a less-pronounced conductance peak around $10^{-4.5}G_0$, which suggests the existence of small amounts of molecules in the oxidized state at the transition potential. We note that although the conductance change induced by adjusting the electrode potential is relatively small in the redox-inactive potential region, as compared to the change taking place as the potential crosses the redox peak potential, it is still comparable to those of several other previously studied molecular switches.[4a,23]

To enable a more precise comparison between the experiments (Figure 4a,b) and the calculations, we plotted the calculated transmission using the electrochemical energy

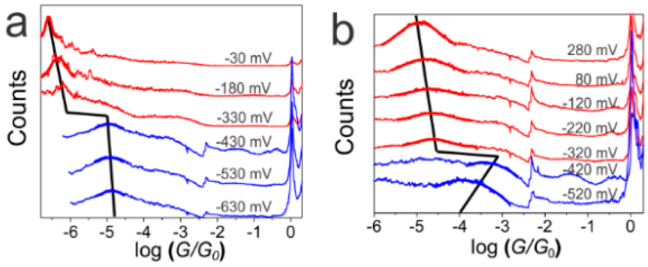

Figure 3. Conductance histograms obtained at different potentials vs SCE for (a) AQ-1,5 and (b) AQ-1,4. Black lines indicate the conductance changes with electrode potential.

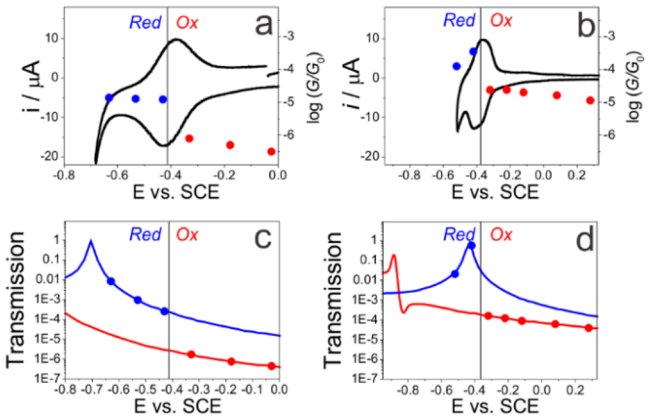

Figure 4. Experimental (a,b) and calculated (c,d) molecular conductance as a function of the applied gating potential vs SCE for AQ-1,5 (a,c) and AQ-1,4 (b,d). The vertical gray line indicates the measured redox potential for the two molecules. The transmission curves shown in the lower panels are the same as in Figure 2, but are plotted here on the electrochemical energy scale relative to SCE.

scale relative to SCE in Figure 4c,d. Conversion of the electrochemical energy scales is achieved based on the Fermi level in the transport calculations corresponding to the (negative) work function of Au(111), which is taken to be 5.3 eV, while the SCE is 4.68 eV relative to vacuum.[24] The gray line indicates the measured redox potentials. For potentials to the left of the gray line, the molecule is in the reduced state and the transmission is given by the blue curve. For potentials to the right of the dashed line, the molecule is in the oxidized state and the transmission is given by the red curve. The dots indicate the predicted conductance at the potentials used to produce the experimental conductance curve in Figure 4a,b. The striking agreement between the calculations and experiments strongly supports the interpretations of the conduction mechanisms put forward in this paper and suggests that (semi)quantitative modeling of single-molecule transport under electrochemical control is possible using relatively simple computational models. Finally, we note that although the qualitative agreement between theory and experiments is excellent, there are significant differences at the quantitative level, in particular for the reduced states. We ascribe this to an incorrect level alignment in the DFT+Sigma calculation for reduced AQ-1,4 and a breakdown of the phase-coherent transport mechanism close to the resonance in the case of reduced AQ-1,5 (see SI for a more detailed discussion).

In summary, we have studied charge transport through single-molecule junctions formed by two isomeric AQ-based derivatives, AQ-1,5 and AQ-1,4, by employing an STM-BJ

dx.doi.org/10.1021/ja510335z | J. Am. Chem. Soc. 2014, 136, 17922−17925

technique under electrochemical control. For both AQ-1,5 and AQ-1,4, the conductance has been controlled over 1 order of magnitude by varying the electrode potential over a range of ∼1 V. In the redox-inactive potential region, the effect of the gating is to shift the Fermi level relative to the molecular resonances, leading to a modest change in conductance. At the redox potential, large and reversible jumps of the conductance were observed due to the change in redox state, which is accompanied by changes in the conjugation pattern from linear (in the reduced state) to cross-conjugated (in the oxidized state). All these observations were supported by our DFT-based transport calculations. In particular, we found an excellent agreement between experiments and calculations for the conductance versus gate potential both outside and inside the redox-active regimes.

■ ASSOCIATED CONTENT

Supporting Information

Synthetic procedures, computational, and single-molecule measurement details. This material is available free of charge via the Internet at http://pubs.acs.org.

■ AUTHOR INFORMATION

Corresponding Authors

hong@dcb.unibe.ch
thygesen@fysik.dtu.dk
m.r.bryce@durham.ac.uk

Author Contributions

#M.B., X.Z., and K.B.Ø contributed equally to this work.

Notes

The authors declare no competing financial interest.

■ ACKNOWLEDGMENTS

We acknowledge discussions with Prof. Hans Siegenthaler and Prof. Silvio Decurtins. This work was generously supported by the Swiss National Science Foundation (200020-144471; NFP 62), the EC FP7 ITN "MOLESCO" project no. 606728, the Scientific Exchange Programme NMSch (SciEx 13.060), FP7 project ACMOL (618082), and the University of Bern. K.B.Ø. and K.S.T. thank the Danish Council for Independent Research's DFF Sapere Aude program (grant no. 11-1051390) for financial support.

■ REFERENCES

(1) van der Molen, S. J.; Liao, J.; Kudernac, T.; Agustsson, J. S.; Bernard, L.; Calame, M.; van Wees, B. J.; Feringa, B. L.; Schoenenberger, C. *Nano Lett.* **2009**, *9*, 76.

(2) Lortscher, E.; Ciszek, J. W.; Tour, J.; Riel, H. *Small* **2006**, *2*, 973.

(3) Song, H.; Kim, Y.; Jang, Y. H.; Jeong, H.; Reed, M. A.; Lee, T. *Nature* **2009**, *462*, 1039.

(4) (a) Kay, N. J.; Higgins, S. J.; Jeppesen, J. O.; Leary, E.; Lycoops, J.; Ulstrup, J.; Nichols, R. J. *J. Am. Chem. Soc.* **2012**, *134*, 16817. (b) Ricci, A. M.; Calvo, E. J.; Martin, S.; Nichols, R. J. *J. Am. Chem. Soc.* **2010**, *132*, 2494.

(5) (a) Haiss, W.; van Zalinge, H.; Higgins, S. J.; Bethell, D.; Hobenreich, H.; Schiffrin, D. J.; Nichols, R. J. *J. Am. Chem. Soc.* **2003**, *125*, 15294. (b) Pobelov, I. V.; Li, Z.; Wandlowski, T. *J. Am. Chem. Soc.* **2008**, *130*, 16045.

(6) Chen, F.; He, J.; Nuckolls, C.; Roberts, T.; Klare, J. E.; Lindsay, S. *Nano Lett.* **2005**, *5*, 503.

(7) (a) Xiao, X.; Brune, D.; He, J.; Lindsay, S.; Gorman, C. B.; Tao, N. *Chem. Phys.* **2006**, *326*, 138. (b) Zhou, X.-S.; Liu, L.; Fortgang, P.; Lefevre, A.-S.; Serra-Muns, A.; Raouafi, N.; Amatore, C.; Mao, B.-W.; Maisonhaute, E.; Schoellhorn, B. *J. Am. Chem. Soc.* **2011**, *133*, 7509.

(8) Albrecht, T.; Guckian, A.; Kuznetsov, A. M.; Vos, J. G.; Ulstrup, J. *J. Am. Chem. Soc.* **2006**, *128*, 17132.

(9) Li, C.; Mishchenko, A.; Li, Z.; Pobelov, I.; Wandlowski, T.; Li, X. Q.; Würthner, F.; Bagrets, A.; Evers, F. *J. Phys.: Condens. Matter* **2008**, *20*, No. 374122.

(10) Della Pia, E. A.; Chi, Q.; Jones, D. D.; Macdonald, J. E.; Ulstrup, J.; Elliott, M. *Nano Lett.* **2011**, *11*, 176.

(11) Tsoi, S.; Griva, I.; Trammell, S. A.; Blum, A. S.; Schnur, J. M.; Lebedev, N. *ACS Nano* **2008**, *2*, 1289.

(12) Leary, E.; Higgins, S. J.; van Zalinge, H.; Haiss, W.; Nichols, R. J.; Nygaard, S.; Jeppesen, J. O.; Ulstrup, J. *J. Am. Chem. Soc.* **2008**, *130*, 12204.

(13) Capozzi, B.; Chen, Q.; Darancet, P.; Kotiuga, M.; Buzzeo, M.; Neaton, J. B.; Nuckolls, C.; Venkataraman, L. *Nano Lett.* **2014**, *14*, 1400.

(14) (a) Markussen, T.; Stadler, R.; Thygesen, K. S. *Nano Lett.* **2010**, *10*, 4260. (b) Garcia-Suarez, V. M.; Lambert, C. J.; Manrique, D. Z.; Wandlowski, T. *Nanotechnology* **2014**, *25*, No. 205402. (c) Xia, J.; Capozzi, B.; Wei, S.; Strange, M.; Batra, A.; Moreno, J. R.; Amir, R. J.; Amir, E.; Solomon, G. C.; Venkataraman, L.; Campos, L. M. *Nano Lett.* **2014**, *14*, 2941. (d) Arroyo, C. R.; Tarkuc, S.; Frisenda, R.; Seldenthuis, J. S.; Woerde, C. H. M.; Eelkema, R.; Grozema, F. C.; van der Zant, H. S. J. *Angew. Chem., Int. Ed.* **2013**, *52*, 3152. (e) Darwish, N.; Diez-Perez, I.; Da Silva, P.; Tao, N.; Gooding, J. J.; Paddon-Row, M. N. *Angew. Chem., Int. Ed.* **2012**, *51*, 3203. (f) Guedon, C. M.; Valkenier, H.; Markussen, T.; Thygesen, K. S.; Hummelen, J. C.; van der Molen, S. J. *Nat. Nanotechnol.* **2012**, *7*, 304.

(15) Valkenier, H.; Guedon, C. M.; Markussen, T.; Thygesen, K. S.; van der Molen, S. J.; Hummelen, J. C. *Phys. Chem. Chem. Phys.* **2014**, *16*, 653.

(16) Hong, W.; Valkenier, H.; Meszaros, G.; Manrique, D. Z.; Mishchenko, A.; Putz, A.; Garcia, P. M.; Lambert, C. J.; Hummelen, J. C.; Wandlowski, T. *Beilstein J. Nanotechnol.* **2011**, *2*, 699.

(17) (a) Li, Z.; Pobelov, I.; Han, B.; Wandlowski, T.; Blaszczyk, A.; Mayor, M. *Nanotechnology* **2007**, *18*, No. 044018. (b) Weibel, N.; Grunder, S.; Mayor, M. *Org. Biomol. Chem.* **2007**, *5*, 2343. (c) Li, C.; Mishchenko, A.; Li, Z.; Pobelov, I.; Wandlowski, T.; Li, X. Q.; Wuerthner, F.; Bagrets, A.; Evers, F. *J. Phys.: Condens. Matter* **2008**, *20*, No. 374122.

(18) (a) Hong, W.; Manrique, D. Z.; Moreno-Garcia, P.; Gulcur, M.; Mishchenko, A.; Lambert, C. J.; Bryce, M. R.; Wandlowski, T. *J. Am. Chem. Soc.* **2012**, *134*, 2292. (b) Li, C.; Pobelov, I.; Wandlowski, T.; Bagrets, A.; Arnold, A.; Evers, F. *J. Am. Chem. Soc.* **2008**, *130*, 318.

(19) Enkovaara, J.; Rostgaard, C.; Mortensen, J. J.; Chen, J.; Dulak, M.; Ferrighi, L.; Gavnholt, J.; Glinsvad, C.; Haikola, V.; Hansen, H. A.; Kristoffersen, H. H.; Kuisma, M.; Larsen, A. H.; Lehtovaara, L.; Ljungberg, M.; Lopez-Acevedo, O.; Moses, P. G.; Ojanen, J.; Olsen, T.; Petzold, V.; Romero, N. A.; Stausholm-Moller, J.; Strange, M.; Tritsaris, G. A.; Vanin, M.; Walter, M.; Hammer, B.; Hakkinen, H.; Madsen, G. K. H.; Nieminen, R. M.; Norskov, J. K.; Puska, M.; Rantala, T. T.; Schiotz, J.; Thygesen, K. S.; Jacobsen, K. W. *J. Phys.: Condens. Matter* **2010**, *22*, 253202.

(20) Mowbray, D. J.; Jones, G.; Thygesen, K. S. *J. Chem. Phys.* **2008**, *128*, 111103.

(21) Quek, S. Y.; Venkataraman, L.; Choi, H. J.; Louie, S. G.; Hybertsen, M. S.; Neaton, J. B. *Nano Lett.* **2007**, *7*, 3477.

(22) (a) Hoft, R. C.; Ford, M. J.; Garcia-Suarez, V. M.; Lambert, C. J. *J. Phys.: Condens. Matter* **2008**, *20*, No. 025207. (b) Schelhaas, M.; Glomsda, S.; Hansler, M.; Jakubke, H. D.; Waldmann, H. *Angew. Chem., Int. Ed.* **1996**, *35*, 106.

(23) Li, Z.; Li, H.; Chen, S.; Froehlich, T.; Yi, C.; Schönenberger, C.; Calame, M.; Decurtins, S.; Liu, S.-X.; Borguet, E. *J. Am. Chem. Soc.* **2014**, *136*, 8867.

(24) Trasatti, S. *Pure Appl. Chem.* **1986**, *58*, 955.